Towards Optimal Binary Patterns for Compressive Terahertz Single-Pixel Imaging

Adolphe Ndagijimana*, Iñigo Ederra*, and Miguel Heredia Conde†
*Antennas Group, Public University of Navarre, Pamplona, Spain
†Center for Sensor Systems (ZESS), University of Siegen, Siegen, Germany
adolphe.ndagijimana@unavarra.es, inigo.ederra@unavarra.es, and heredia@zess.uni-siegen.de

***Abstract*—Terahertz (THz) radiation's properties make it ideal for various imaging applications. However, creating simple, cost-effective, and high-resolution THz array detectors is challenging. Mechanical scanning is commonly used but creates a trade-off between frame rate and resolution. Fortunately, Compressive Sensing (CS) offers a solution by reducing the required number of measurements needed compared to Shannon-Nyquist's sampling theory. CS-THz imaging is usually implemented using a single-pixel camera with spatial modulation patterns, mostly binary patterns. However, the non-uniform and diffraction propagation present in the THz range affects the mutual coherence of the resulting sensing matrices resulting in image reconstruction degradation. In this paper, we introduce an optimization procedure for generating binary patterns that consider THz diffraction and non-uniform illumination of the mask. The produced sensing matrices exhibit low coherence compared to other typical binary sensing matrices, resulting in a higher reconstruction performance than all others.**

***Index Terms*—Compressive Sensing, Single pixel camera, Terahertz wave propagation**

I. Introduction

Terahertz(THz) radiation, ranging from 0.1 to 10 THz, has great potential for imaging and material characterization. Despite the fact that its full potential has been compromised by the lack of sources and detectors, various electronic and photonic technologies are recently being adapted to develop THz radiation sources and detectors [1]. This development has opened up multiple opportunities for applications. THz radiation's unique energy level and wavelength allow it to interact with matter at different levels, making it an essential tool for material characterization. THz radiation can penetrate most daily objects and tools like plastics and clothes while being reflected by conducting materials. However, it is absorbed by water. Due to it being non-ionizing, THz radiation is ideal for surveillance, security screening, and non-destructive inspection [2], [3].

THz imaging faces the challenge of lack of cost-effective high-resolution array detectors. The traditional approach of pixel-by-pixel mechanical scanning or mechanical scanning with low-resolution array detectors creates a trade-off between scanning time and attainable resolution.

Compressive sensing (CS) reduces the number of required measurements dictated by the Shannon-Nyquist sampling theorem [4]. The most popular implementation of CS is the single pixel camera, which utilizes a single detector to detect modulated radiations [5]–[7]. Different patterns spatially modulate the THz wavefront during each acquisition, allowing measurements according to different sensing functions for the same scene at the detector. CS exploits signal sparsity or compressibility within specific domains. Achieving accurate signal reconstruction requires adherence to the Restricted Isometry Property (RIP) by the sensing matrix. However, verifying the RIP with tight constants is not feasible, leading to using mutual coherence as a practical substitute.

CS recovery methods enable the reconstruction of sparse signals with s non-zero coefficients, provided that the number of measurements m equals or exceeds a required minimum that is typically $O(s\ \log n)$. Notably, the minimum number of measurements depends on several factors, including the reconstruction method, the mutual coherence of the sensing matrix, and the signal's sparsity [8].

A multitude of signals possess inherent sparsity or compressibility in specific domains. Moreover, there are multiple CS recovery techniques available [4], [9]–[13]. Low-coherence sensing matrices are easily accessible and can be directly implemented in particular disciplines, such as optics. Still, the nature of THz radiation, dictated by its wavelength, which produces diffraction, poses a challenge [14]. It is important to consider the physical effects of using THz radiation for CS recovery. Non-uniform illumination caused by the usual Gaussian beam characteristics of THz sources radiation and diffraction effects due to the mask pixel size in terms of wavelength significantly impact the commanded mask, leading to variations in the THz mask patterns with respect to the commanded mask. This, in turn, influences the mutual coherence of the sensing matrix.

Different researchers have indicated that decreasing coherence can enhance the effectiveness of radar systems. In [15], authors aimed to create unimodular sequences with beneficial correlations to lower integrated slight levels, consequently increasing the merit factor. In [16], the authors emphasized the significance of considering the reconstruction technique when designing wavefronts for CS Radar, explicitly highlighting the importance of coherence minimization. Moreover, in [17], positioning antenna elements to minimize coherence has been found to improve target detection capabilities.

In our previous study [18], we have thoroughly investigated

This project has received funding from the European Union's Horizon 2020 research and innovation programme under the Marie Skłodowska-Curie grant agreement No 860370

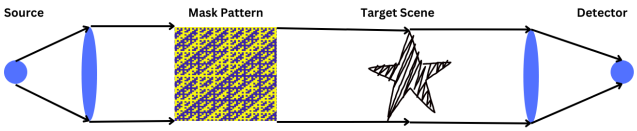

Fig. 1: Refractive THz single pixel camera

the impact of diffracted propagation on commonly used CS sensing matrices, such as Hadamard, random Gaussian, random Bernoulli, Low-Density Parity Check (LDPC) Codes, and Best Antipodal Spherical Codes (BASCs), in CS-THz imaging. Our focus was on the influence of diffraction and mutual coherence on the quality of THz imaging. Our results showed the necessity of considering THz radiation diffraction and unique characteristics when designing sensing matrices. We have now taken this further by introducing a groundbreaking method to develop a set of binary sensing mask patterns that produce optimal sensing matrices by seeking minimal coherence. This approach requires fewer measurements and significantly enhances accuracy compared to traditional binary sensing matrices like LDPC, random Bernoulli, and Hadamard sensing matrices.

II. Mutual coherence of THz imaging system

Due to the unavailability of cost-effective array detectors, a single-pixel detector is traditionally used to scan an object mechanically point by point. This creates a trade-off between the attainable frame rate and image resolution. Ongoing research contemplates using a single-pixel camera [19] that permits high-resolution images at a high frame rate by omitting direct mechanical scanning [20]. This is achieved through spatial modulation of THz radiation, and when combined with CS, it reduces the number of required measurements, permitting a high frame rate.

Different factors must be considered when designing a THz imaging system to ensure signal recoverability. Figure 1 depicts a THz single-pixel camera in a refractive configuration. THz radiation is generated at the source, then modulated with a spatial light modulator, and interacts with the scene before being collected by the detector. Note that the modulation can happen before, as in Figure 1, after, or before and after interaction with the scene. Since direct spatial light modulators are not available in the THz range, the radiation is typically obtained by translating the optical spatial modulation from a digital micromirror device (DMD) or a liquid crystal display (LCD) into modulation of the THz radiation through a chosen semiconductor [21]. When illuminated with low-wavelength energy, semiconductors modify the refractive index of the illuminated area, enabling modulation of the incident THz radiation. In [22], they demonstrated that also the phase is modulated before amplitude modulation.

To reconstruct an image, $\vec{x} \in \mathbb{C}^n$, from measurements, $\vec{y} \in \mathbb{C}^m$, obtained by projecting different mask patterns onto the scene, a measurement matrix $\Phi \in \mathbb{C}^{m \times n}$ must be obtained; this linear transformation Φ relates the measurement $\vec{y}$ to the image $\vec{x}$. Due to the quasi-optical properties of the radiation of THz sources [23] and the wavelength of THz radiation being in the same range as the dimension of mask pixels, the commanded mask at the spatial light modulator differs from the measurement mask. This affects the properties of the sensing matrix, such as the mutual coherence, which is an important factor for assuring the signal reconstruction for a given number of measurements when using CS methods.

As in the system design displayed in Fig. 1, we would like to develop a linear transform that relates the measurement and the target image. The THz source radiation is generated and propagated from the modulator to the mask, with $\vec{E}_{\mathrm{T_xM}}$ modelled using quasioptics. The THz field at the mask is then modulated by the SLM ($\vec{E}_{\mathrm{mask}} = \vec{E}_{\mathrm{T_xM}} \odot m_i$), diffracts to the scene with D_{ms} modelled with [24], and interacts with the scene ($\vec{E}_{\mathrm{scene}} = \vec{x} \odot (D_{ms}\vec{E}_{\mathrm{mask}})$). This electric field then diffracts and is collected by the detector with diffracted propagation matrix, D_{MRx}, resuting in the corresponding measurement $y_i = \sum_{i=1}^{n} D_{\mathrm{MRx}}(\vec{E}_{\mathrm{scene}})$. This can be summarized as $\vec{y} = \Phi\vec{x}$, with Φ defined as the measurement matrix:

$$\Phi = MD \text{ with } D = D_{\mathrm{ms}}^{T}\mathrm{diag}\left(\vec{E}_{\mathrm{T_xM}}\right) D_{\mathrm{MR_x}} \tag{1}$$

The analysis of CS THz setups involves the use of the coherence matrix $A = [\vec{a_i}]_i^m = \Phi\Theta$, with Θ being the dictionary for sparse representation, which is a crucial concept for analysing the minimum number of measurements required for assuring the image reconstruction by CS recovery methods. The coherence $\mu(A)$ determines the effectiveness of the setup; however, it is impacted by the diffracted propagation, D, as shown in (1). To define the concept of mutual coherence mathematically, we use the equation:

$$\mu(A) = \max_{i \neq j, 1 \leq i,j \leq n} \left(\frac{|\vec{a_i}\vec{a_j}|}{\|\vec{a_i}\|_2 \|\vec{a_j}\|_2} \right) \tag{2}$$

When the columns $\vec{a_i}$ are normalized to unit length, the mutual coherence can be expressed in terms of the Gramian matrix $G = A^H A$. The mutual coherence, in this case, is defined as $\mu(A) = \max(|G - I_n|)$, where I_n is the identity matrix of size n. The aim is to minimize the mutual coherence, and this can be achieved by solving the following optimization problem:

$$\min_A \|f(A)\|_F^2 \text{ with } f(A) = A^H A - I_n \tag{3}$$

Different approaches, including the gradient descent method, can be used to obtain a solution. By minimizing the mutual coherence, the performance of the CS THz imaging setup can be improved. A similar method has been applied to obtain a given dictionary's measurement matrices [25], [26].

With a fixed setup, the diffraction propagation matrix D is fixed. Provided that A is a function of M, we want to find the mask M that solves (3):

$$min_M \|f(M)\|_F^2 \text{ with } f(M) = D^H M^H M H - I_n \tag{4}$$

$$\frac{\delta f}{\delta M} = \frac{\delta \|D^H M^H M D - I_n\|_F^2}{\delta M} \tag{5}$$

By solving as in (5),

$$\frac{\delta f}{\delta M} = 4MD\left(D^H M^H MD - I_n\right)D^H \tag{6}$$

Note that in the case the signal is not sparse by nature but can obtain sparsity or compressibility in dictionary Θ, the matrix D is expressed as a linear combination $D \times \Theta$, and hence we assume sparsity of the signal.

We can add projection to the sparse reprojection error on (4), as shown in [27]. This results in the minimization equation:

$$\min_M \|M\|_F^2 + \|D^H M^H MD - I_n\|_F^2 \tag{7}$$

Additionally, the gradient of the function becomes:

$$\frac{\delta f}{\delta M} = 4MD\left(D^H M^H MD - I_n\right)D^H + 2M \tag{8}$$

The minimum attainable coherence depends on the number of measurements and signal dimension, $\mu(A) \geq \mu_{\min}(m,n) := \sqrt{\frac{n-m}{m(n-1)}}$. This is taken into account in the minimization process. Instead of using the identity matrix, we can define a matrix H that takes into consideration $\mu_{\min}(m,n)$.

$$H = \begin{cases} g_{ij}, & \text{when } i \neq j \text{ and } |g_{ij}| \leq \mu_{\min} \\ \mu_{\min}, & \text{when } i \neq j \text{ and } |g_{ij}| > \mu_{\min} \\ 1, & \text{otherwise} \end{cases} \tag{9}$$

There are two important considerations for the gradient descent algorithm: first, we are optimizing a binary matrix M, which is different from previous assumptions of $M \in \mathbb{C}^{m\times n}$. Instead, M is binary $M \in \{b_1, b_2\}^{m\times n}$, and an extra step is required to ensure projection to the binary set of values; for example, we use hyperbolic tangent for assuring convergence to $\{-1, 1\}$. Secondly, the columns of the sensing matrix A are not always normalized by a selection of M values; and depending on the columns of D, normalization using selection of an adequate M for it may not be possible. Therefore, we need to normalize the columns of A and perform a thresholding step to obtain M as a binary matrix. The resulting optimization is summarized in Algorithm 1. Similar to other gradient descent algorithms, A proper selection of K, L, and β, representing the number of steps for the gradient step for each H, the number of steps of updating the matrix H and the step size for each gradient update of M respectively, is necessary.

III. Results and Discussion

When using single pixel THz imaging to create high-quality images of a target scene, having a sensing matrix with low mutual coherence is of great importance. This is because the sensing matrix generated from propagation can differ from the commanded masks when the target scene is not in the near field. Continuous sensing matrices, such as random Gaussian sensing matrices, are limited by the SLM's number of bits used for quantization. Therefore, binary sensing matrices, such as random Bernoulli and Hadamard, are commonly used. Our research explores the optimal implementation of binary sensing matrices to reduce mutual coherence.

Input: $m, D, \beta, \mu_{min}, K, L$
Result: Optimized M
Initialize M to a random matrix;
Initialize H to an identity matrix;
for $l = 1$ *to* L **do**
  $A = \text{sign}(M)D$;
  $\overline{A} = \text{diag}\left(\left[\frac{1}{\|(\vec{a})_i\|_2}\right]_{i=1}^{n}\right)A$;
  $G = \overline{A}^H\overline{A}$;
  foreach $i \neq j$ **do**
    $h_{ij} = g_{ij}$ if $|g_{ij}| < \mu_{min}$, otherwise
    $h_{ij} = \mu_{min}$;
  end
  for $k = 1$ *to* K **do**
    $A = \text{sign}(M)D$;
    $\overline{A} = \text{diag}\left(\left[\frac{1}{\|\vec{a}_i\|_2}\right]_{1=1}^{n}\right)A$;
    $G = \overline{A}^H\overline{A}$;
    $M = M - \beta(M\left(\text{diag}\left(\left[\frac{1}{\|d_i\|_2}\right]_{i=1}^{n}\right)D\right)(G -$
    $H)\left(\text{diag}\left(\left[\frac{1}{\|d_i\|_2}\right]_{i=1}^{n}\right)D\right)^H + 0.5M)$;
    $M = \tanh(M)$;
  end
end
$M = \text{sign}(M)$

Algorithm 1: Commanded matrix optimization

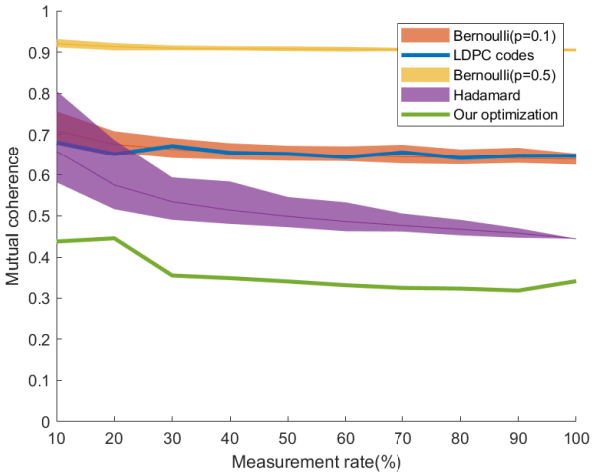

Fig. 2: Comparison of resulting coherence of our proposed matrix for THz binary sensing optimization with commonly used single-pixel matrices at various measurement rates ($\frac{m}{n}$).

Figure 2 displays the coherence of different binary sensing matrices at a specific sampling level. This is based on a mask positioned 100 mm from the source, with a target scene located 102 mm from the mask and a collecting lens situated 100 mm from the scene. The scene dimensions are set to $n = 1024$ pixels, with a pixel dimension in both the x and y-axis being twice the wavelength. The source generates a frequency of 750 GHz. To obtain the Hadamard matrices, we randomly select 100 random column selection experiments at each sampling rate, while for the Bernoulli matrix, we generate 100 random sensing matrices for each step as well. The resulting coherence can differ from that of the original commanded masks in the optical domain on the SLM.

The random Bernouilli matrices [28], consisting of $\{0, 1\}$, allow for spatial modulation by enabling the mask pixel semiconductor region optically illuminated to be transparent to THz and the non-illuminated to block the THz radiation. The coherence is affected by diffraction and pixel density, with a lower p, the probability of getting 1, resulting in lower coherence but at the cost of high blockage of THz illumination. We compare the system's response in Figure 2 at $p = 0.1$ and $p = 0.5$. The low-density parity-check (LDPC) [29] codes also exhibit low density and coherence in binary sensing matrices based on amplitude modulation by allowing or blocking THz illumination.

Hadamard sensing matrices [30] are binary, using values of {-1,1}. By selecting random columns of the Hadamard sensing matrix, their corresponding THz sensing matrices show low coherence compared to binary sensing matrices based on amplitude modulation. In addition to having low coherence, there do not block THz radiation like the other masks presented above.

In our optimization, we developed a range of sensing matrices at varying sampling rates $\left(\frac{m}{n}\right)$, all of which were acquired using the setup described in Figure 1. To generate binary matrices based on phase modulation, meaning each pixel value $\in \{-1, 1\}$, we employed the minimization technique outlined in Algorithm 1. Our results, Figure 2, showed that the coherence resulting from this optimization technique exceeded that of all the other sensing matrices across all sampling rates, thus demonstrating its superior effectiveness.

To assess the reconstruction performance of the sensing matrix, we conducted a simulation using multiple examples from the MNIST dataset, resizing them to obtain 1024 pixel points. The results, shown in Figure 3, show the average performance across 100 random examples at each sampling rate (m/n) using Orthogonal Matching Pursuit (OMP) [13]. Our sensing matrix outperformed all other sensing matrices across all sampling rates, as evaluated using the structure similarity, peak-to-noise ratio, and root mean square error metrics. This can also be checked by a visual representation of reconstruction in Figure 4. Hence, it illustrates the superiority of using matrices with minimal coherence and the importance of our developed method for coherence minimization for sparse reconstruction.

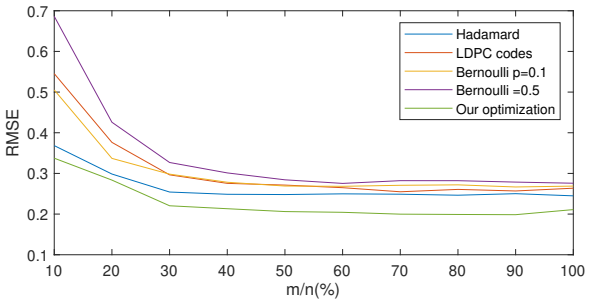

(a) Root Mean Square Error (RSME)

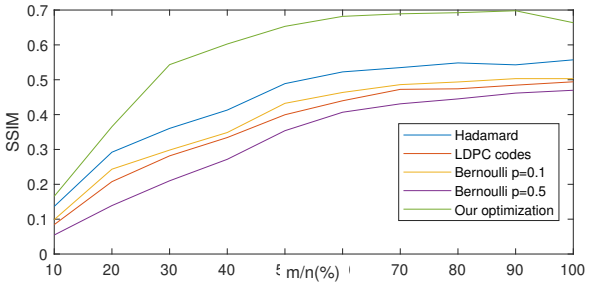

(b) Structure Similarity(SSIM)

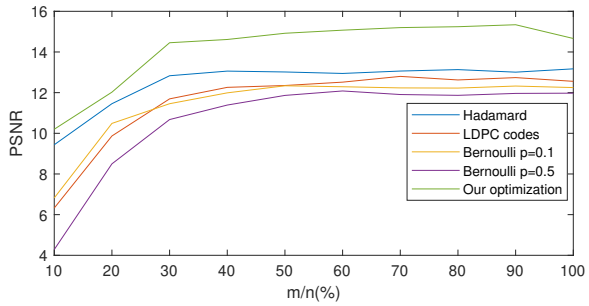

(c) Peak Signal to Noise Ration (PSNR)

Fig. 3: Comparison of different binary sensing matrices performance in reconstructing images in a simulation of the single pixel CS THz imaging system refractive setup, Figure 1, with the MNIST images dataset serving as the target scene. The matrices tested were random Bernoulli matrices with varying p-values, LDPC codes, random columns of the Hadamard matrix, and our optimization technique that minimizes mutual coherence.

IV. Conclusion

In single-pixel CS-THz imaging, diffraction and non-uniform illumination can significantly impact the resulting sensing matrix. Changes in mutual coherence can adversely affect the successful recovery of THz images using compressive sensing recovery algorithms. Although binary sensing patterns are typically used to create the sensing matrix, the diffraction and non-uniformity of THz radiation increase the mutual coherence of the matrix compared to the desired one, thereby reducing signal reconstruction quality.

We have introduced a coherence-based approach for single-

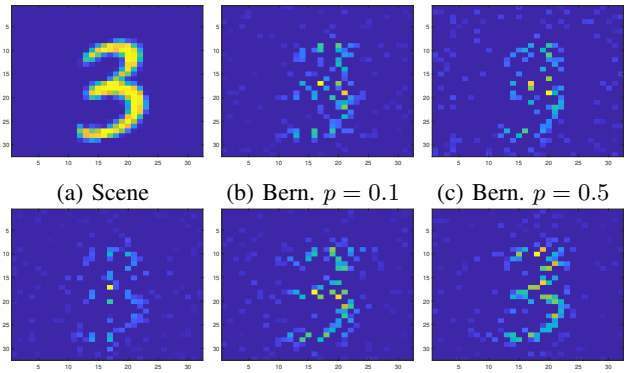

(a) Scene (b) Bern. $p = 0.1$ (c) Bern. $p = 0.5$

(d) LDPC codes (e) Hadamard (f) Our optimization

Fig. 4: Reconstruction example using $\frac{m}{n} = 30\%$ measurements using the single-pixel CS THz imaging system refractive setup, Figure 1. Note that the sampling theorem dictates that to retrieve the signal at least n measurements are required. Bern. stands for the random Bernoulli sensing matrices.

pixel CS THz imaging that optimises THz sensing matrices based on binary sensing patterns. Our optimization process has generated low-coherency sensing matrices that have demonstrated superior imaging reconstruction quality compared to all other binary sensing matrices considered using CS sparse recovery methods. By leveraging our approach, we can ensure more accurate and reliable THz imaging, boosting its applicability across a wide range of applications.

ACKNOWLEDGMENT

This project has received funding from the European Union's Horizon 2020 research and innovation program under the Marie Skłodowska-Curie grant agreement No 860370.

REFERENCES

[1] H.-J. Song and T. Nagatsuma, *Handbook of terahertz technologies: devices and applications*. CRC press, 2015.

[2] D. Woolard, R. Brown, M. Pepper, and M. Kemp, "Terahertz frequency sensing and imaging: A time of reckoning future applications?," *Proceedings of the IEEE*, vol. 93, no. 10, pp. 1722–1743, 2005.

[3] I. Amenabar, F. Lopez, and A. Mendikute, "In introductory review to thz non-destructive testing of composite mater," *Journal of Infrared, Millimeter, and Terahertz Waves*, vol. 34, pp. 152–169, 2013.

[4] E. J. Candès and M. B. Wakin, "An introduction to compressive sampling," *IEEE signal processing magazine*, vol. 25, no. 2, pp. 21–30, 2008.

[5] W. L. Chan, K. Charan, D. Takhar, K. F. Kelly, R. G. Baraniuk, and D. M. Mittleman, "A single-pixel terahertz imaging system based on compressed sensing," *Applied Physics Letters*, vol. 93, no. 12, 2008.

[6] R. I. Stantchev, D. B. Phillips, P. Hobson, S. M. Hornett, M. J. Padgett, and E. Hendry, "Compressed sensing with near-field thz radiation," *Optica*, vol. 4, no. 8, pp. 989–992, 2017.

[7] S. Augustin, P. Jung, S. Frohmann, and H.-W. Hübers, "Terahertz dynamic aperture imaging at standoff distances using a compressed sensing protocol," *IEEE Transactions on Terahertz Science and Technology*, vol. 9, no. 4, pp. 364–372, 2019.

[8] M. Heredia Conde, *Compressive sensing for the photonic mixer device*. Springer, 2017.

[9] D. Needell and J. A. Tropp, "Cosamp: Iterative signal recovery from incomplete and inaccurate samples," *Applied and computational harmonic analysis*, vol. 26, no. 3, pp. 301–321, 2009.

[10] A. Beck and M. Teboulle, "A fast iterative shrinkage-thresholding algorithm for linear inverse problems," *SIAM journal on imaging sciences*, vol. 2, no. 1, pp. 183–202, 2009.

[11] T. Blumensath and M. E. Davies, "Iterative hard thresholding for compressed sensing," *Applied and computational harmonic analysis*, vol. 27, no. 3, pp. 265–274, 2009.

[12] H. Mohimani, M. Babaie-Zadeh, and C. Jutten, "A fast approach for overcomplete sparse decomposition based on smoothed ℓ_0 norm," *IEEE Transactions on Signal Processing*, vol. 57, no. 1, pp. 289–301, 2008.

[13] Y. C. Pati, R. Rezaiifar, and P. S. Krishnaprasad, "Orthogonal matching pursuit: Recursive function approximation with applications to wavelet decomposition," in *Proceedings of 27th Asilomar conference on signals, systems and computers*, pp. 40–44, IEEE, 1993.

[14] M. Burger, J. Föcke, L. Nickel, P. Jung, and S. Augustin, "Reconstruction methods in thz single-pixel imaging," in *Compressed Sensing and Its Applications: Third International MATHEON Conference 2017*, pp. 263–290, Springer, 2019.

[15] P. Stoica, H. He, and J. Li, "New algorithms for designing unimodular sequences with good correlation properties," *IEEE Transactions on Signal Processing*, vol. 57, no. 4, pp. 1415–1425, 2009.

[16] L. Anitori and J. Ender, "Waveform design for sparse signal processing in radar," in *2021 IEEE Radar Conference (RadarConf21)*, pp. 1–6, IEEE, 2021.

[17] S. Nagesh, J. Ender, and M. A. González-Huici, "Array position optimisation for compressed sensing mimo radar based on mutual coherence minimisation," in *2022 23rd International Radar Symposium (IRS)*, pp. 98–103, IEEE, 2022.

[18] A. Ndagijimana, M. Heredia Conde, and I. E. Urzainqui, "Performance evaluation of spatial modulation patterns in compressive sensing terahertz imaging," in *2022 IEEE Sensors*, pp. 1–4, IEEE, 2022.

[19] M. F. Duarte, M. A. Davenport, D. Takhar, J. N. Laska, T. Sun, K. F. Kelly, and R. G. Baraniuk, "Single-pixel imaging via compressive sampling," *IEEE signal processing magazine*, vol. 25, no. 2, pp. 83–91, 2008.

[20] D. Shrekenhamer, C. M. Watts, and W. J. Padilla, "Terahertz single pixel imaging with an optically controlled dynamic spatial light modulator," *Optics express*, vol. 21, no. 10, pp. 12507–12518, 2013.

[21] A. Kannegulla, M. I. B. Shams, L. Liu, and L.-J. Cheng, "Photo-induced spatial modulation of thz waves: opportunities and limitations," *Optics express*, vol. 23, no. 25, pp. 32098–32112, 2015.

[22] T. F. Gallacher, R. Sondena, D. A. Robertson, and G. M. Smith, "Optical modulation of millimeter-wave beams using a semiconductor substrate," *IEEE transactions on microwave theory and techniques*, vol. 60, no. 7, pp. 2301–2309, 2012.

[23] J.-L. Coutaz, F. Garet, and V. Wallace, *Principles of Terahertz time-domain spectroscopy*. CRC Press, 2018.

[24] V. Katkovnik, A. Migukin, and J. Astola, "Backward discrete wave field propagation modeling as an inverse problem: toward perfect reconstruction of wave field distributions," *Applied optics*, vol. 48, no. 18, pp. 3407–3423, 2009.

[25] M. Elad, "Optimized projections for compressed sensing," *IEEE Transactions on Signal Processing*, vol. 55, no. 12, pp. 5695–5702, 2007.

[26] V. Abolghasemi, S. Ferdowsi, and S. Sanei, "A gradient-based alternating minimization approach for optimization of the measurement matrix in compressive sensing," *Signal Processing*, vol. 92, no. 4, pp. 999–1009, 2012.

[27] T. Hong and Z. Zhu, "An efficient method for robust projection matrix design," *Signal Processing*, vol. 143, pp. 200–210, 2018.

[28] E. J. Candes and T. Tao, "Near-optimal signal recovery from random projections: Universal encoding strategies?," *IEEE transactions on information theory*, vol. 52, no. 12, pp. 5406–5425, 2006.

[29] R. Gallager, "Low-density parity-check codes," *IRE Transactions on information theory*, vol. 8, no. 1, pp. 21–28, 1962.

[30] J. Hadamard, "Resolution d'une question relative aux determinants," *Bull. des sciences math.*, vol. 2, pp. 240–246, 1893.